coatings

Supplementary Materials: Enhanced Removal of Non-Steroidal Inflammatory Drugs from Water by Quaternary Chitosan-Based Magnetic Nanosorbents

Sofia F. Soares, Tito Trindade and Ana L. Daniel-da-Silva *

CICECO-Aveiro Institute of Materials, Department of Chemistry, University of Aveiro, 3810-193 Aveiro, Portugal; sofiafsoares@ua.pt (S.F.S.); tito@ua.pt (T.T.)
* Correspondence: ana.luisa@ua.pt; Tel.: +351-234-401-518

1. Experimental

1.1. Synthesis of Fe_3O_4 Nanoparticles

Ultra-pure water was first deoxygenated with N_2 under vigorous stirring for two hours. Then, 25 mL of deoxygenated water was added to a 250 mL round flask, and 1.90 g and 1.52 g of KOH and KNO_3 were added, respectively. The mixture was heated at 60 °C with bubbling N_2 and mechanically stirred at 500 rpm. After salt dissolution, 25 mL of deoxygenated water containing 4.75 g of $FeSO_4.7H_2O$ was added drop-by-drop, and the stirring was increased to 700 rpm for 30 min. After the reaction, the flask was transferred to an oil bath at 90 °C and left without stirring for 4 h, under N_2. The resulting black powder was washed several times with deoxygenated water and ethanol and magnetically separated. Then, the Fe_3O_4 nanoparticles were dried by evaporating the solvent at room temperature.

1.2. Synthesis of SiO_2 Nanoparticles

Briefly, 4.5 mL of deionized water, 42.5 mL of ethanol, and 0.75 mL of ammonia solution were mixed with the 2.25 mL of TEOS at room temperature (25 °C) under constant stirring (250–300 rpm). The reaction was performed over 24 h, and the resulting SiO_2 particles were washed thoroughly with deionized water and ethanol, followed by centrifugation. The solvents were evaporated, and amorphous SiO_2 particles were obtained.

2. NSAIDs

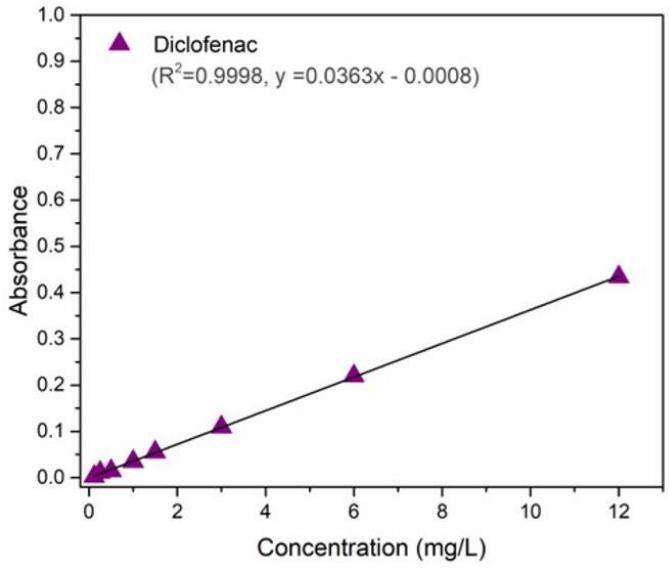

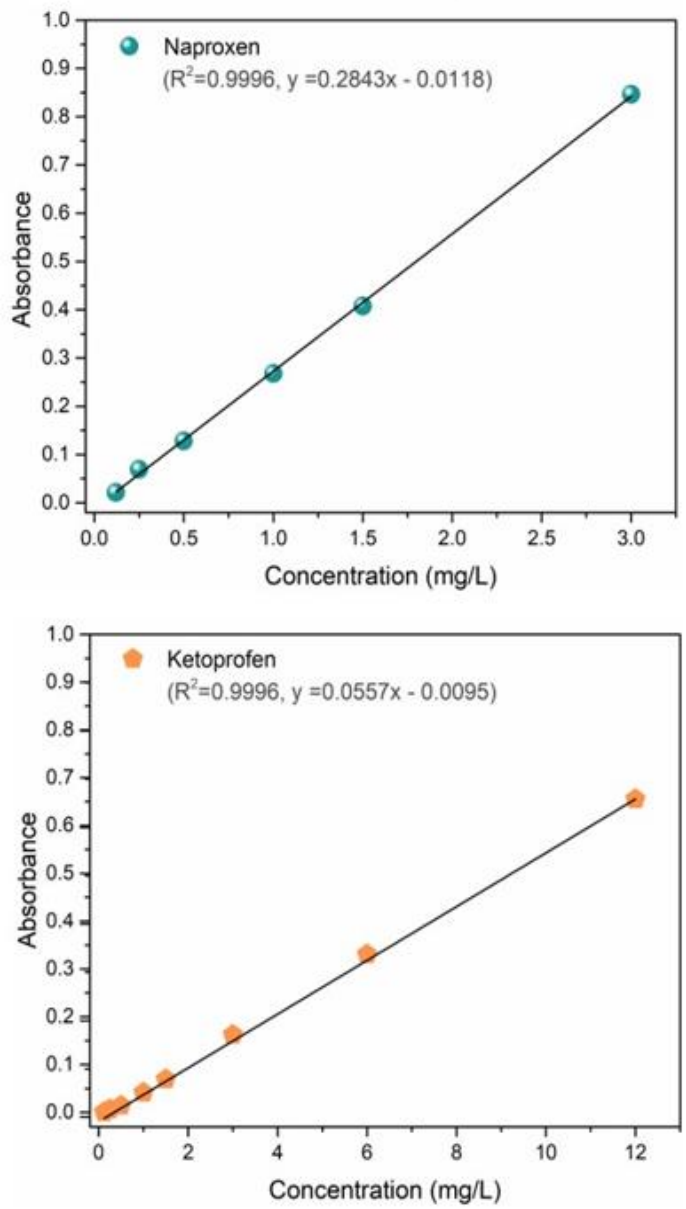

Figure S1. Calibration curves for diclofenac (0.12–12.0 mg/L), naproxen (0.12–3 mg/L), and ketoprofen (0.12–12.0 mg/L) in ultra-pure water, providing a linear relation between the absorbance and the concentration.

Table S1. Selected characteristics and structures of NSAIDs [1,2].

Compound	Diclofenac Sodium	Naproxen Sodium	Ketoprofen
Molecular structure	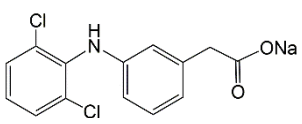	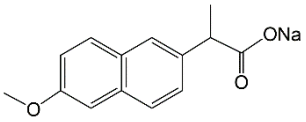	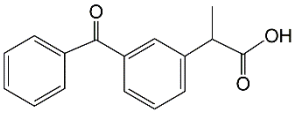
Chemical formula	$C_{14}H_{11}Cl_2NNaO_2$	$C_{14}H_{13}NaO_3$	$C_{16}H_{14}O_3$
Molecular weight	318.13 g/mol	252.24 g/mol	254.28 g/mol
pKa	4.00	4.19	4.45
λ (max)	276 nm	230 nm	260 nm

3. Particle Characterization

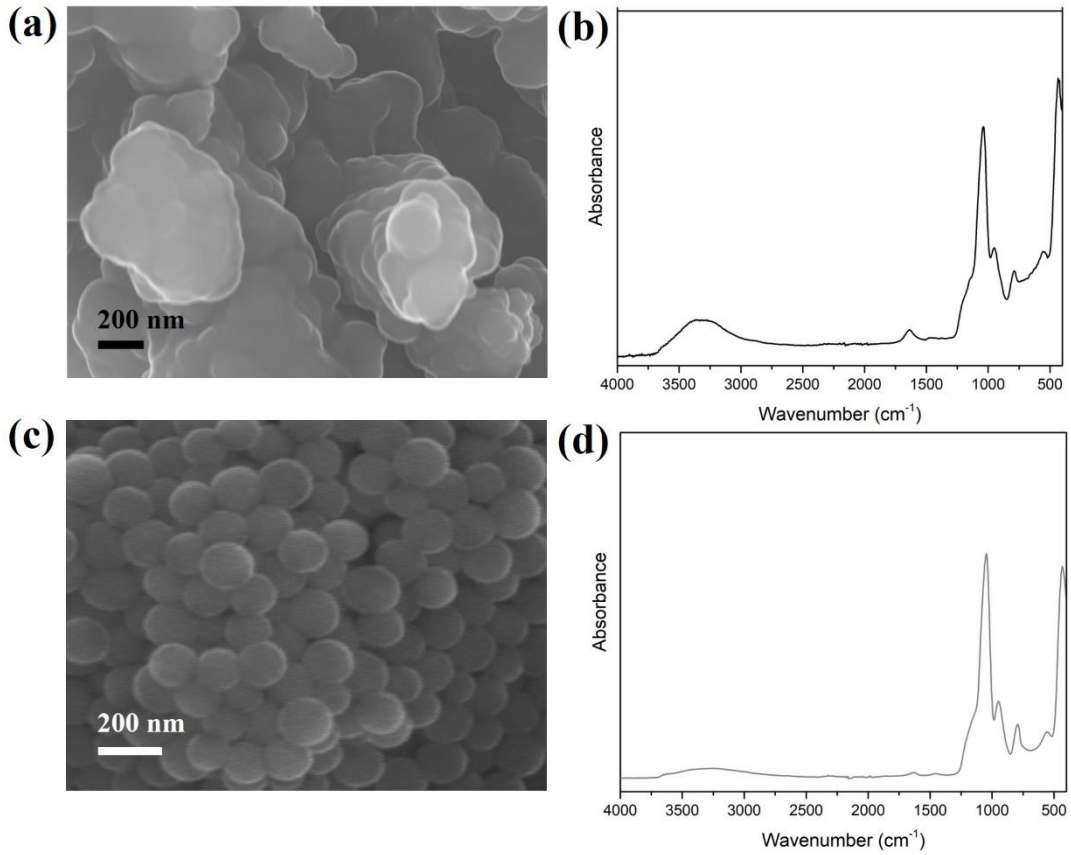

Figure S2. SEM images of (**a**) SiO_2/TMC/GPTMS and (**c**) SiO_2 particles and ATR-FTIR spectra of (**b**) SiO_2/TMC/GPTMS and (**d**) SiO_2 particles.

Table S2. ^{13}C CP/MAS, ^{29}Si MAS, and ^{29}Si CP/MAS NMR chemical shifts for TMC, SiO_2/TMC/GPTMS, and SiO_2 particles, and quantification of the ^{29}Si Q^n resonances.

^{13}C CP/MAS			^{29}Si MAS			^{29}Si CP/MAS		
Resonance assignment	**TMC**	**SiO_2/TMC/ GPTMS**	**Resonance assignment**	**SiO_2**	**SiO_2/TMC/GPTMS**	**Resonance assignment**	**SiO_2**	**SiO_2/TMC/ GPTMS**
C_1	99.7	104.1	Q^2	–94.4 (1.0%)	–91.9 (3.0%)	Q^2	–91.2	–91.6
C_2 C_6	57.8	61.1	Q^3	–102.2 (33.4%)	–101.2 (29.7%)	Q^3	–101.3	–101.5
C_3 C_5	74.7	74.8	Q^4	–111.3 (65.4%)	–111.3 (68.1%)	Q^4	–111.3	–111.3
C_4	81.1	83.7	–	–	–	T^2	–	–57.6
Acetyl groups	24.3/ 173.8	22.8/ 173.8	–	–	–	T^3	–	–64.2
$N(CH_3)_2$	54.8	54.8	–	–	–	–	–	–
$N(CH_3)_3$	55.2	57.1	–	–	–	–	–	–
C_a C_b	–	22.8	–	–	–	–	–	–
C_c C_d C_e	–	74.8	–	–	–	–	–	–
C_f	–	61.1	–	–	–	–	–	–

4. Uptake of NSAIDs

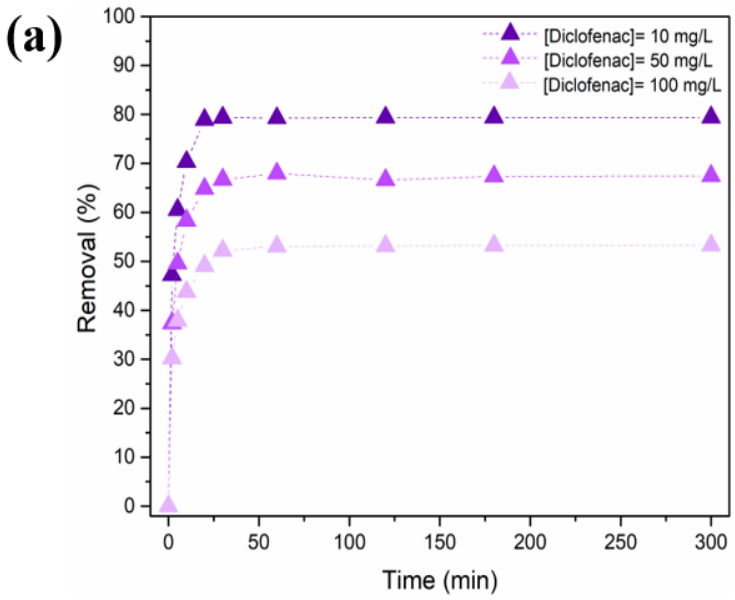

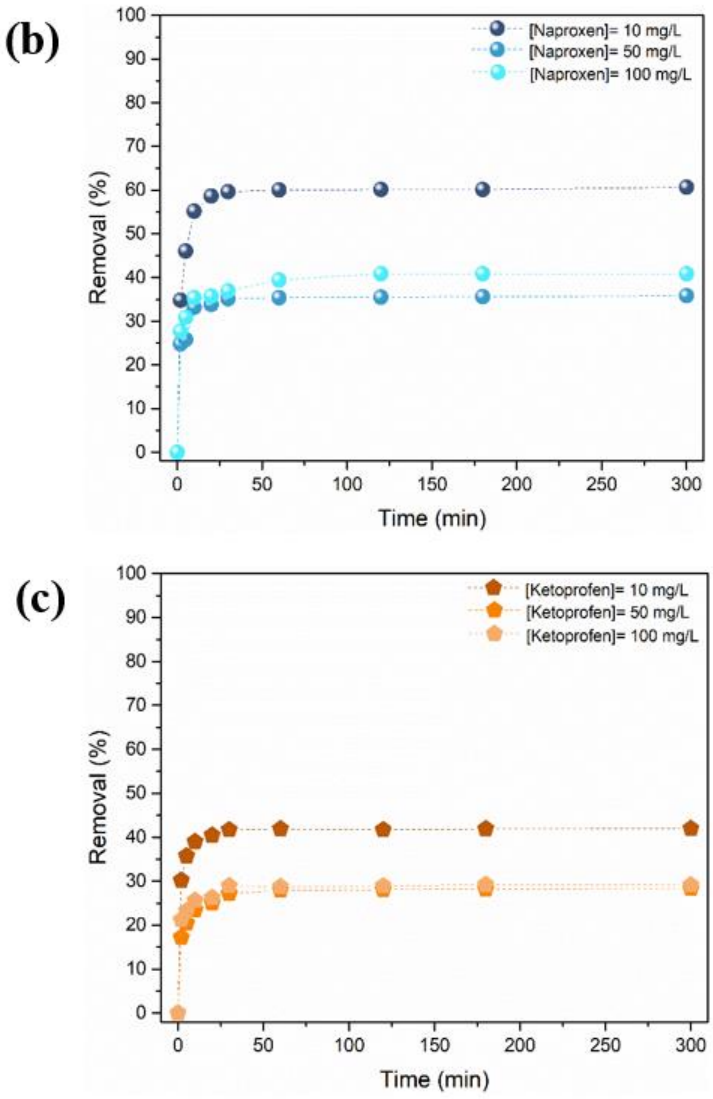

Figure S3. Time profile of removal percentage of NSAIDs at variable (**a**) DCF, (**b**) NAP and (**c**) KET initial concentration (10, 50 and 100 mg/L) using the particles Fe_3O_4@SiO_2/TMC/GPTMS, for 5h (300 min).

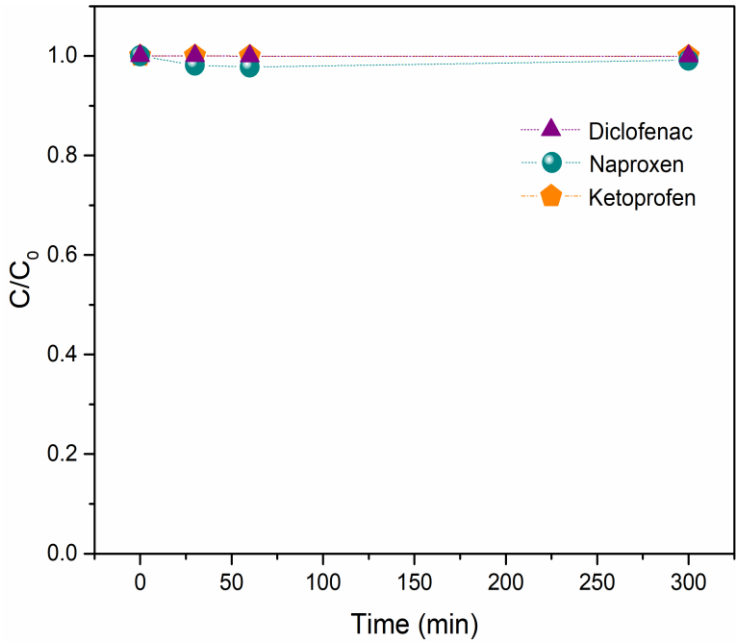

Figure S4. Variation of diclofenac, naproxen and ketoprofen concentration on control experiments performed in absence of adsorbent particles to assess the loss of DCF, NAP and KET caused by other phenomena than adsorption on sorbents.

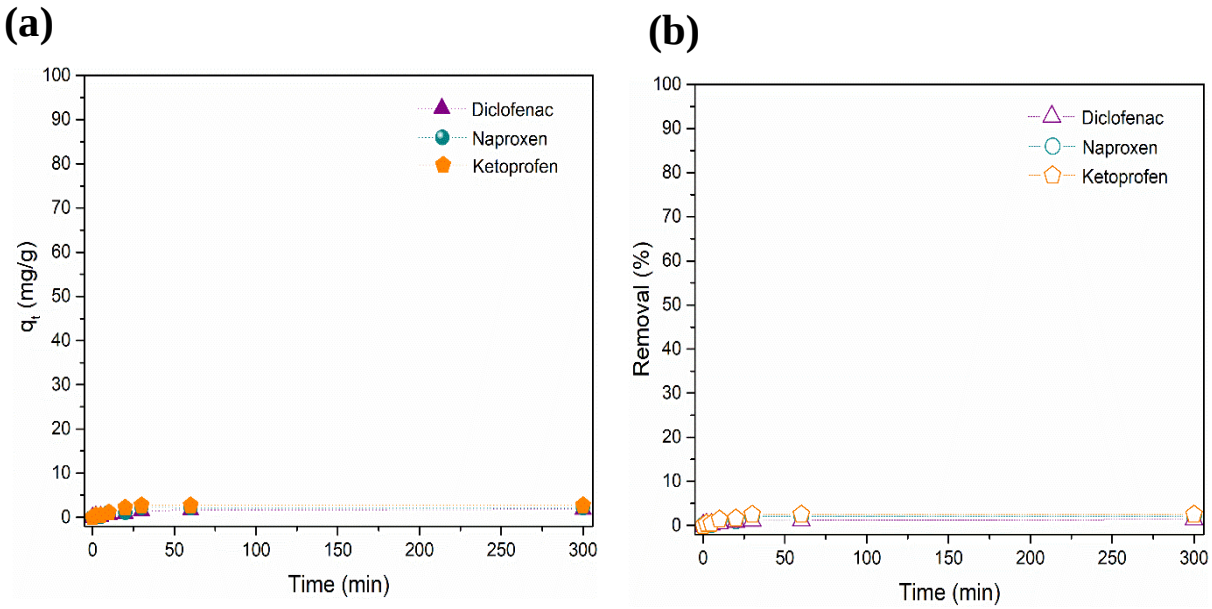

Figure S5. (**a**) Time profile of removal percentage and (**b**) adsorption capacity of diclofenac, naproxen and ketoprofen at 50 mg/L using Fe_3O_4 particles, for 5 h (300 min).

5. Kinetics Modeling and Goodnesses of Fit

Several kinetic models have been established to facilitate the understanding of the adsorption kinetics and determine the rate-limiting step of the sorption process. The corresponding equations are detailed below:

A non-linear form of the pseudo-first kinetic model is given by Equation (S1), where k_1 (min^{-1}) is the pseudo-first order rate constant [3].

$$q_t = q_e(1 - e^{-k_1 t}) \quad \text{(S1)}$$

A non-linear form of the pseudo-second kinetic model is given by Equation (S2), where k_2 (g.mg^{-1}.min^{-1}) is the pseudo-second order rate constant [4].

$$q_t = \frac{k_2 q_e^2 t}{1 + k_2 q_e t} \quad (S2)$$

The Elovich model is given by Equation (S3), where α is the initial adsorption rate (mg.g^{-1}.min^{-1}), and β (mg.g^{-1}.min^{-1}) is the desorption constant [5].

$$q_t = \frac{1}{\beta}\ln(\alpha\beta) + \frac{1}{\beta}\ln(t) \quad (S3)$$

The goodness of fit was evaluated by calculating the coefficient of determination (R^2) and Chi-square test value (χ^2), expressed by Equations (S4) and (S5), respectively:

$$R^2 = 1 - \frac{\sum_{i=1}^{n}(y_i - \hat{y}_i)^2}{\sum_{i=1}^{n}(y_i - \bar{y})^2} \quad (S4)$$

$$\chi^2 = \sum_{i=1}^{n}\frac{(y_i - \hat{y}_i)^2}{\hat{y}_i} \quad (S5)$$

where y_i and $\hat{y}_i$ are the experimental and model predicted values, respectively, $\bar{y}$ is the mean of the experimental data, and n is the sample size.

Table S2. Kinetic parameters estimated from pseudo-first and -second order and Elovich models, and evaluation of its fittings for diclofenac, naproxen, and ketoprofen using Fe_3O_4@SiO_2/TMC/GPTMS particles.

Kinetic Model		Diclofenac			Naproxen			Ketoprofen		
		C_0 = 10 mg/L	**C_0 = 50 mg/L**	**C_0 = 100 mg/L**	**C_0 = 10 mg/L**	**C_0 = 50 mg/L**	**C_0 = 100 mg/L**	**C_0 = 10 mg/L**	**C_0 = 50 mg/L**	**C_0 = 100 mg/L**
Pseudo-first order	R^2 (χ^2)	0.9808 (0.39)	0.9807 (10.55)	0.9636 (41.42)	0.9876 (0.39)	0.9553 (9.26)	0.9519 (30.46)	0.9865 (0.13)	0.9542 (6.50)	0.9619 (16.31)
	k_1 (min^{-1})	0.3759	0.3327	0.3296	0.3693	0.481	0.5366	0.6097	0.3905	0.6268
	q_e (mg.g^{-1})	13.21	67.21	96.70	16.37	42.06	73.37	9.23	34.37	60.83
Pseudo-second order	R^2 (χ^2)	0.9959 (0.08)	0.9972 (1.52)	0.9951 (5.56)	0.9973 (0.08)	0.9849 (3.11)	0.9864 (8.58)	0.9994 (0.01)	0.9919 (1.14)	0.9899 (4.31)
	k_2 (mg.g^{-1}.min^{-1})	0.0491	0.0082	0.0054	0.038	0.0205	0.012	0.1283	0.018	0.0180
	q_e (mg.g^{-1})	13.74	70.16	101.28	17.03	43.63	76.46	9.52	35.99	63.08
Elovich	R^2 (χ^2)	0.9487 (1.06)	0.9473 (28.87)	0.9630 (42.14)	0.9405 (1.69)	0.9666 (6.90)	0.9915 (5.37)	0.9786 (0.20)	0.9770 (3.25)	0.9863 (5.86)
	α	9030.67	12175.50	10169.49	9063.83	212566.6	132269.08	326202.1	7907.84	177557.1
	β	1.02	0.1795	0.1180	0.8101	0.3678	0.1935	2.15	0.3535	0.2820

6. Equilibrium Isotherm Modeling and Goodness of Fit

An equilibrium study on adsorption provided information about the distribution of adsorbate molecules between the liquid and solid phases. Several mathematical models were used to describe the experimental data of the adsorption isotherms. In this work, the most widely used adsorption isotherm models were fit to the experimental data.

Langmuir isotherm*:* widely used for the adsorption of different compounds from aqueous solutions, assuming that adsorbate molecules form a monolayer on the adsorbent surface, which contains a specific number of identical sites [6]. The non-linear form of the Langmuir model is given by Equation (S6) as follows:

$$q_e = \frac{q_L K_L C_e}{1 + K_L C_e} \quad (S6)$$

where q_L (mg/g) is the monolayer adsorption capacity per unit of adsorbent, and K_L (L/mg) is the Langmuir adsorption constant related to the affinity of binding sites.

Freundlich isotherm: an empirical equation describing the adsorption on heterogeneous adsorbents, resulting in adsorption sites of varying energy. This model assumes that the adsorption can occur based on multiple layers [7]. The non-linear form of the Freundlich model is described by Equation (S7) as follows:

$$q_e = k_F {C_e}^{1/n} \quad (S7)$$

where k_F ($mg^{(1-1/n)}.L^{(1/n)}.g^{-1}$) is the Freundlich constant, and 1/n is the heterogeneity factor, which varies between 0 and 1.

Sips isotherm*:* also known as the Langmuir–Freundlich isotherm, combines Langmuir and Freundlich behaviors [8]. At high adsorbate concentration, the Sips equation predicts a monolayer adsorption that is characteristic of the Langmuir isotherm. At low adsorbate concentration, the Sips equation reduces to the Freundlich model. The non-linear form of the Sips model is given by Equation (S8):

$$q_e = \frac{K_S {C_e}^{\beta s}}{1 + a_S {C_e}^{\beta s}} \quad (S8)$$

where Ks (mg/g)·(L/mg) is related to the median binding affinity, a_S (L/mg) is the total number of binding sites, and β_S ($0 < \beta_S < 1$) is the Sips isotherm model exponent.

Goodness of fit was evaluated by calculating the coefficient of determination (R^2) and Chi-square test value (χ^2), expressed by Equations (S4) and (S5), respectively. The model parameters and goodness of fit are depicted in Tables S3–S5.

Table S3. Equilibrium model parameters obtained from model fitting to experimental sorption data of Fe_3O_4@SiO_2/TMC/GPTMS for the removal of DCF, NAP, and KET, together with the goodness of fit.

Isotherm	**Model Parameters**			**Goodness of Fit**	
Langmuir	**q_L (mg/g)**	**K_L (L/mg)**		**R^2**	**χ^2**
DCF	188.57	0.01515		0.9845	50.41
NAP	438.15	0.00421		0.9692	126.8
KET	221.57	0.00667		0.9858	50.79
Freundlich	**K_F ($mg^{(1-1/n)}$ $L^{(1/n)}$ g^{-1})**	**n**		**R^2**	**χ^2**
DCF	12.52	2.18		0.9610	126.89
NAP	5.34	1.46		0.9833	68.6
KET	4.82	1.64		0.9628	133.64
Sips	**K_S (mg/g).(L/mg)**	**a_S (L/mg)**	**βs**	**R^2**	**χ^2**
DCF	0.01373	178.26	0.9643	0.9858	57.44
NAP	0.0000045	402.98	0.68504	0.9820	68.6
KET	0.0013	275.54	0.65295	0.9944	22.91

Reference

1. ChemIDplus advanced, (n.d.). https://chem.nlm.nih.gov/chemidplus/ (accessed 20 September 2020).
2. Mlunguza, N.Y.; Ncube, S.; Mahlambi, P.N.; Chimuka, L.; Madikizela, L.M. Adsorbents and removal strategies of non-steroidal anti-inflammatory drugs from contaminated water bodies. *J. Environ. Chem. Eng.* **2019**, 7, 103142. doi:10.1016/j.jece.2019.103142.

3. Lagergren, S. Zur theorie der sogenannten adsorption gelöster stoffe. *Zeitschr f Chem und Ind der Kolloide* 2. **1907,** 15. https://doi.org/10.1007/BF01501332.
4. Ho, Y.S.; McKay, G. Pseudo-second order model for sorption processes. *Process Biochem.* **1999**, 34, 451–465. doi:10.1016/S0032-9592(98)00112-5.
5. Chien, S.H.; Clayton, W.R. Application of Elovich equation to the kinetics of phosphate release and sorption in soils. *Soil Sci. Soc. Am. J*. **1980**, 44, 265. doi:10.2136/sssaj1980.03615995004400020013x.
6. Langmuir, I. The adsorption of gases on plane surfaces of glass, mica and platinum. *J. Am. Chem. Soc.* **1918**, 40, 1361–1403. doi:10.1021/ja02242a004.
7. Freundlich, H.Z. Concerning adsorption in solutions. *Zeitschrift Für Phys. Chemie.* **1906**, 57, 444–448.
8. Sips, R. On the structure of a catalyst surface. *J. Chem. Phys.* **1948**, 16, 490. doi:10.1063/1.1746922.